Vol. 9, No. 5 May 1999

GSA TODAY

A Publication of the Geological Society of America

INSIDE

- Promoting Geoscience Education, p. 11
- GSA Divisions, p. 18
- Committee Opportunities, p. 20

Stressed Rock Strains Groundwater at Yucca Mountain, Nevada

David A. Ferrill, James Winterle, Gordon Wittmeyer, Darrell Sims, Shannon Colton, Amit Armstrong, *Center for Nuclear Waste Regulatory Analyses, Southwest Research Institute, 6220 Culebra Rd., San Antonio, TX 78238-5166*

Alan P. Morris, *Division of Earth and Physical Sciences, University of Texas, San Antonio, TX 78249*

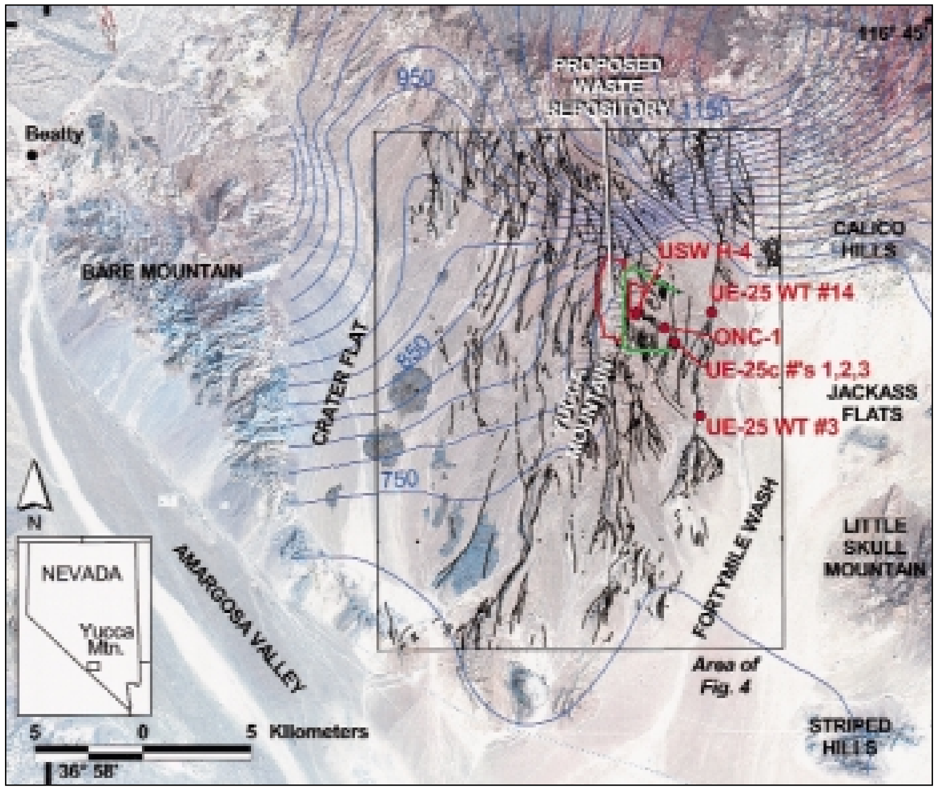

Figure 1. Thematic Mapper scene with potential repository location, wells (red dots), faults (irregular black lines), and water-table contours (blue lines). Water-table contours are from Czarnecki et al. (1997). Green line shows path of Exploratory Studies Facility.

ABSTRACT

Groundwater flow at Yucca Mountain, Nevada, must be understood to determine transport and dilution of contaminants released from the proposed high-level waste repository. The nature of such flow in a complexly faulted and fractured tuff aquifer is not easily characterized. Conceptual models of regional groundwater flow often assume isotropic transmissivity, resulting in flow being interpreted as parallel to the gradient of the potentiometric surface. However, fractured aquifers are typically anisotropic, their transmissivity controlled by the conductive properties of faults and fractures, which are partially controlled by the in situ stress field. Faults at Yucca Mountain predominantly strike approximately north (azimuth ~005). Slip and dilation tendency analysis of the region indicates that those faults and fractures ideally oriented for slip in the current stress field strike north-northeast (azimuth ~025–030) and dip moderately to steeply, whereas those ideally oriented for dilation strike north-northeast (azimuth ~025–030) and are vertical. Faults with favorable orientations for slip or dilation present potential fluid flow pathways. These observations imply anisotropic transmissivity at Yucca Mountain with an azimuthal direction of maximum transmissivity between 005 (based on dominant fault trend) and 030 (based on slip- and dilation-tendency constraints). Reinterpretation of data from a long-term aquifer pumping test on the eastern flank of Yucca Mountain indicates anisotropic transmissivity with a maximum principal transmissivity direction of approximately 030. This is consistent with anisotropic transmissivity controlled by faults and fractures active in the present-day in situ stress field.

INTRODUCTION

Yucca Mountain, a faulted east-dipping cuesta of Miocene tuffs in southwestern Nevada, is being evaluated as the potential site for the nation's first permanent repository for high-level radioactive waste (Fig. 1). The U.S. Department of Energy has prepared a viability assessment, which provides a characterization of the proposed repository, including descriptions of geologic setting, design, and long-term (10 000 year) performance (U.S. Department of Energy, 1998a, 1998b). The Department of Energy is expected to submit a license application in 2002. If the site is licensed by the U.S. Nuclear Regulatory Commission, high-level waste could be emplaced as early as 2010. Original consideration of Yucca Mountain as the candidate repository site was due in part to the >500-m-thick unsaturated zone beneath the mountain and the dry climate. These environmental characteristics were expected to inhibit release and transport of contaminants to the accessible environment via groundwater flow.

Permeability in the Miocene welded tuffs and the underlying Paleozoic and Precambrian carbonate and clastic strata at Yucca Mountain and surrounding area is primarily controlled by faults and fractures (Waddell, 1982; Winograd and Thordarson, 1975; Fridrich et al., 1994). On the basis of alignment of springs (e.g., Ash

Stressed Rock *continued on p. 2*

GSA TODAY

Vol. 9, No. 5 **May 1999**

GSA TODAY (ISSN 1052-5173) is published monthly by The Geological Society of America, Inc., with offices at 3300 Penrose Place, Boulder, Colorado. Mailing address: P.O. Box 9140, Boulder, CO 80301-9140, U.S.A. Periodicals postage paid at Boulder, Colorado, and at additional mailing offices. Postmaster: Send address changes to *GSA Today,* Membership Services, P.O. Box 9140, Boulder, CO 80301-9140.

SUBSCRIPTIONS for 1999 calendar year: Society Members: *GSA Today* is provided as part of membership dues. Contact Membership Services at (800) 472-1988, (303) 447-2020 or member@geosociety.org for membership information. Nonmembers & Institutions: Free with paid subscription to both *GSA Bulletin* and *Geology,* otherwise $50 for U.S., Canada, and Mexico; $60 elsewhere. Contact Subscription Services. Single copies may be requested from Publication Sales. Also available on an annual CD-ROM, (together with *GSA Bulletin, Geology,* GSA Data Repository, and an Electronic Retrospective Index to journal articles from 1972); $89 to GSA Members, others call GSA Subscription Services for prices and details. Claims: For nonreceipt or for damaged copies, members contact Membership Services; all others contact Subscription Services. Claims are honored for one year; please allow sufficient delivery time for overseas copies, up to six months.

STAFF: Prepared from contributions from the GSA staff and membership.
Executive Director: ***Donald M. Davidson, Jr.***
Science Editors: ***Suzanne M. Kay,*** *Department of Geological Sciences, Cornell University, Ithaca, NY 14853;* ***Molly F. Miller,*** *Department of Geology, Box 117-B, Vanderbilt University, Nashville, TN 37235*
Forum Editor: ***Bruce F. Molnia,*** *U.S. Geological Survey, MS 917, National Center, Reston, VA 22092*
Director of Publications: ***Peggy S. Lehr***
Managing Editor: ***Faith Rogers***
Assistant Editor: ***Vanessa Carney***
Production Manager: ***Jon Olsen***
Production Editor and Coordinator: ***Gaynor Bloom***
Graphics Production: ***Gaynor Bloom***

Issues of this publication are available as electronic Acrobat files for free download from GSA's Web Site, http://www.geosociety.org. They can be viewed and printed on various personal computer operating systems: MSDOS, MSWindows, Macintosh, and Unix, using the appropriate Acrobat reader. Readers are available, free, from Adobe Corporation: http://www.adobe.com/acrobat/readstep.html.

This publication is included on GSA's annual CD-ROM, *GSA Journals on Compact Disc.* Call GSA Publication Sales for details.

Printed in U.S.A. using pure soy inks.

50% Total Recoverd Fiber
10% Postconsumer

IN THIS ISSUE

Stressed Rock Strains Groundwater at Yucca Mountain, Nevada 1
In Memoriam 2
Penrose Conference: Volcanic Rifted Margins 3
About People 7
GSA International Internet Symposium: An Experiment in Scientific Communication 9
SAGE Remarks 11
1999 GSA Section Meeting 12
Washington Report 14
GSAF Update 16
Letter 17
GSA Divisions—Do You Belong? 18
1999–2000 Section Officers and Past Chairs 19
Committees 20
New Headquarters Department Focuses on Development 24
Book Reviews 24
Field Forums 24
Call for Short Course Proposals 25
2000 Annual Meeting 25
Bulletin and *Geology* Contents 27
Calendar 30
Classifieds 31

In Memoriam

Alan S. Horowitz
Bloomington, Illinois

W. Bradley Meyers
Denver, Colorado

Frank F. Simons
Lakewood, Colorado
January 6, 1995

Stressed Rock *continued from p. 1*

Meadows fault—Winograd and Thordarson, 1975; Dudley and Larson, 1976), and elevated groundwater temperatures along faults (e.g., Midway Valley and Solitario Canyon faults—Sass et al., 1995), studies have concluded that faults control groundwater flow locally and are paths for upward flow in the saturated zone at Yucca Mountain (Fridrich et al., 1994; Bredehoeft, 1997). Anomalous concentrations of ^{36}Cl recently identified in samples from the Exploratory Studies Facility, a 7.8-km-long, 7.6-m-diameter tunnel beneath Yucca Mountain (Fig. 1), have been interpreted as indicating rapid downward transport of meteoric water along faults and fractures in the unsaturated zone (Levy et al., 1997; Fabryka-Martin et al., 1998). The production of ^{36}Cl is largely related to atmospheric nuclear testing in the Pacific Ocean in the 1950s.

Anisotropic permeability in fractured aquifers arises from the abundance and distribution of faults and fractures and permeability of associated damage zones (e.g., breccia) (Fig. 2). Although it is known that faulted and fractured aquifers commonly have anisotropic transmissivity (National Research Council, 1996), maps depicting regional-scale groundwater flow usually assume flow parallel to the gradi-

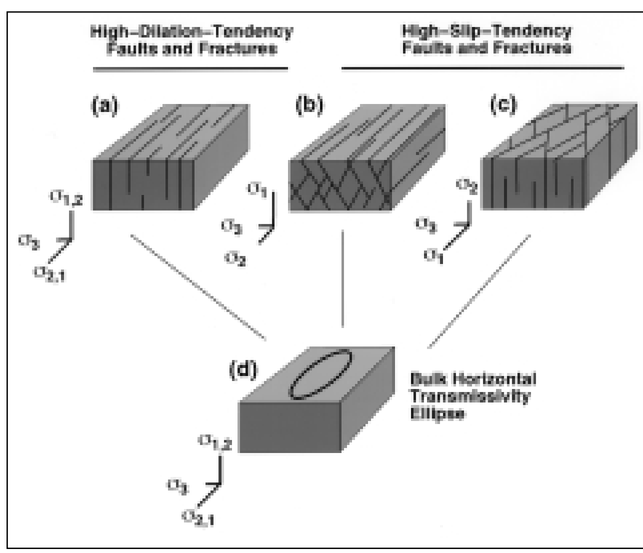

Figure 2. Conceptual illustration of effects of faults with high slip tendency or high dilation tendency on development of anisotropic transmissivity in areas, like the Yucca Mountain (Nevada) region, where the minimum principal compressive stress (σ_3) is horizontal.

PENROSE CONFERENCE

Volcanic Rifted Margins

March 27–31, 2000

Conveners:
Ian Davison and Martin Menzies, Department of Geology, Royal Holloway University;
Joel Baker, Danish Lithosphere Centre

Please note change of venue:
Royal Holloway University of London, Egham Surrey, UK

Conference Purpose and Objectives

Many rifted volcanic margins (<200 m.y. old) are in close proximity to mantle plumes, but the causal relationship between plumes and rifting remains highly controversial. Do plumes drive continental breakup, or are they channeled into areas of thinned lithosphere? In addition, the relative timing of surface uplift, extension, and magmatism has been predicted by theoretical plume models, but their validity hinges on actual field examples. The North Atlantic and southern Red Sea margins appear to have evolved in a similar way, with minimal uplift and much of the flood magmatism pre-dating break-up. Why does this differ from theoretical models? This conference will bring together scientists working on theoretical, field, and geophysical aspects of rifts, in a stimulating environment.

Field- and laboratory-based scientists with diverse areas of expertise, including landscape evolution and geomorphology, the chronology and geochemistry of continental volcanism, lithospheric extension, mantle and crustal geophysics, thermochronology, and theoretical modeling of rift settings, will be invited to the conference. The main topics will include: extent and amount of uplift and subsidence; relative timing of geological processes on volcanic rifted margins; absolute dating techniques for extension, magmatism, and exhumation; use of volcanic products to understand rift geodynamics; style of, and mechanisms for, lithospheric thinning; syn- and postrift exhumation, sediment budgets and basin formation; thermal history of volcanic rifted margins using dating and modeling techniques.

Field Trips

A premeeting six-day trip to the Deccan Traps will cost an estimated $1000, and a postmeeting five-day trip to the Isle of Mull, Scotland, will cost an estimated $650.

Registration

Limited funding will be available to help cover conference expenses for academics from developing countries, young scientists, and graduate students. Early applications are recommended if you are seeking funding. The conference is limited to 80 participants; selection will include a broad range of disciplines. Costs are currently estimated at $400 for the conference. Interested parties should contact Julie Brown (brown@gl.rhbnc.ac.uk); identify the e-mail as "Penrose Conference." Registration deadline is August 31, 1999. Please include in your e-mail a brief statement of your field of interest, relevance of your research work to the conference theme, proposed title of a poster presentation, a title of topic for discussion (maximum 10 minutes, with a maximum of five overhead projections or slides). Let us know whether you would be interested in participating in the field trips. Invitations will be based on your e-mailed application. Participants will be notified on September 14, 1999, by e-mail.

For more information, contact Ian Davison, Royal Holloway, University of London, Egham, Surrey TW20 OEX UK, phone 44-1784-443615, fax 44-1784- 471780, davison@gl.rhbnc.ac.uk. ■

Sue Beggs Retires

After almost 20 years as the Meetings Manager for GSA, Sue Beggs retired in January 1999. She spearheaded the planning and staging of GSA annual meetings ranging from 4,000 to 7,500 attendees.

Beggs is now a meeting planning consultant in Boulder, Colorado. Kathy Ohmie Lynch, who has been with GSA for 25 years, has assumed the directorship of the GSA Meetings Department.

Stressed Rock *continued from p. 2*

ent of the potentiometric surface. This is true only if the transmissive properties of the aquifer are isotropic, or if the major or minor semi-axis of the transmissivity tensor is everywhere parallel to the potentiometric gradient.

Recent studies, including one example from Yucca Mountain, have shown that faults favorably oriented for slip in the ambient stress field tend to be the most active groundwater flow pathways (Barton et al., 1995; Finkbeiner et al., 1997). This observation has been explained by increased small-scale fracturing and faulting in the vicinity of faults on the verge of shear failure (Barton et al., 1995). The ability to recognize such faults allows us to identify the loci of increased fracturing.

A secondary but measurable influence on permeability is the effect of contemporary stress on reducing apertures of existing faults and fractures (Carlsson and Olsson, 1979; Barton et al., 1995; Finkbeiner et al., 1997). Faults and fractures perpendicular to the maximum principal stress are preferentially closed, thereby reducing permeability perpendicular to the maximum principal stress. Permeability perpendicular to the minimum principal compressive stress direction is relatively enhanced because lower resolved normal stress results in less fracture aperture reduction (e.g., Carlsson and Olsson, 1979).

Here, we examine how regional stress combined with existing faults and fracture systems at Yucca Mountain influences permeability and groundwater flow in the saturated zone beneath Yucca Mountain. We then test the model using data from a long-term aquifer pumping test at Yucca Mountain, and consider possible implications for the proposed high-level waste repository at Yucca Mountain.

SLIP TENDENCY AND DILATION TENDENCY

Our approach to stress analysis involves calculating resolved stresses on fault and fracture surfaces to analyze like-

Stressed Rock *continued on p. 4*

Stressed Rock *continued from p. 3*

lihood for slip or dilation in crustal stress fields. The resulting slip and/or dilation tendency data are displayed by color coding three-dimensional models (Fig. 3) or trace maps of the fault and fracture array (Fig. 4).

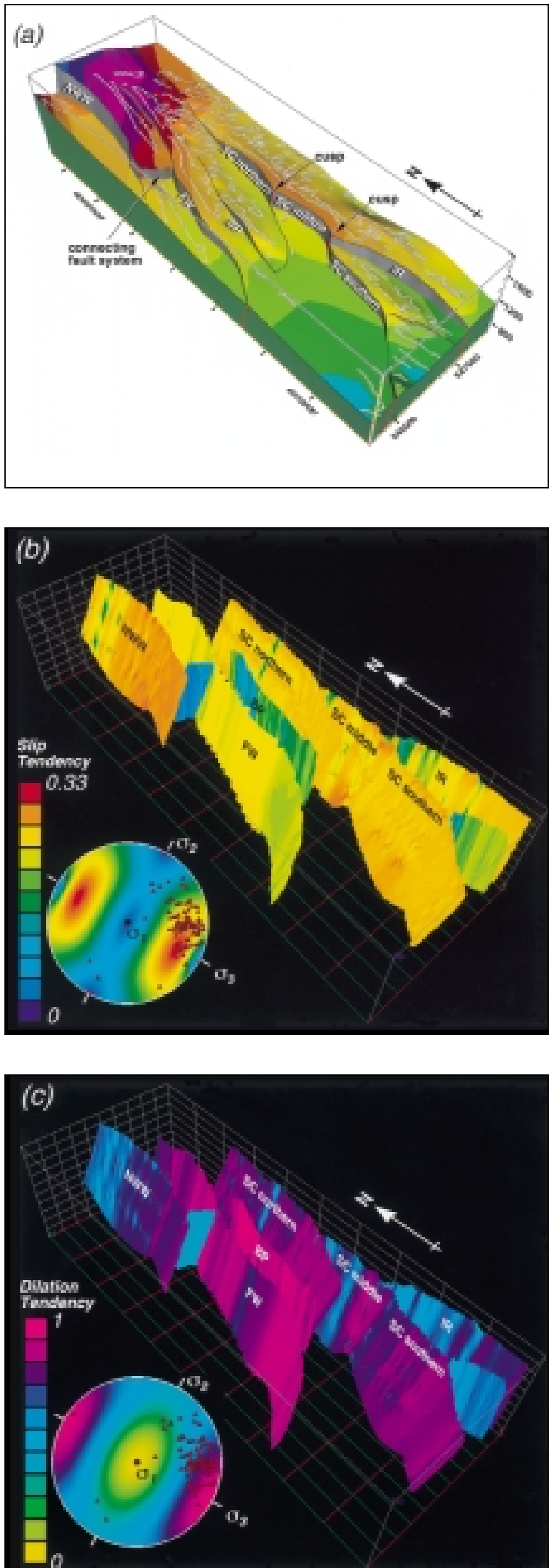

Figure 3. (a) Three-dimensional structure contour map of layer (top of upper lythophysal zone of the crystal-poor member) within the Tiva Canyon Tuff in the western Yucca Mountain, Nevada, area. Irregular white lines represent data points from the three-dimensional outcrop trace of the mapped horizon (from Day et al., 1998a, 1998b). Gray indicates fault gaps for Northern Windy Wash (NWW), Fatigue Wash (FW), Boomerang Point (BP), Solitario Canyon (SC, subdivided into northern, middle, and southern sections), and Iron Ridge (IR) faults. Coordinates are UTM zone 11, elevations are in meters above sea level, and vertical exaggeration is 2.5×. See Figure 4 for location.

(b) Three-dimensional model of western Yucca Mountain fault system with fault surfaces colored according to slip tendency. The slip tendency plot (equal-angle stereographic projection colored according to slip tendency as defined in text) shows poles to planes (measurements from Simonds et al., 1995 and Day et al., 1998a) of the Windy Wash, Fatigue Wash, Boomerang Point, Solitario Canyon, and Iron Ridge faults. The area is the same as in part a; no vertical exaggeration.

(c) Three-dimensional dilation tendency model of western Yucca Mountain fault system. The dilation tendency plot (equal-angle stereographic projection colored according to dilation tendency as defined in text) shows poles to planes of the Windy Wash, Fatigue Wash, Boomerang Point, Solitario Canyon, and Iron Ridge faults. The area is the same as in part a; no vertical exaggeration.

Slip Tendency

Slip tendency analyses are applicable to planar discontinuities like faults, extension fractures, or layering (Morris et al., 1996; Ferrill et al., 1998). For faults and fractures, slip is likely to occur on a surface when the resolved shear stress, τ, on that surface equals or exceeds the frictional resistance to sliding. Frictional resistance is proportional to normal stress, σ_n, acting across that surface (Jaeger and Cook, 1979). The slip tendency, T_s, of a surface is the ratio of shear stress to normal stress acting on that surface (Morris et al., 1996):

$$T_s = \tau / \sigma_n$$

As such, T_s depends solely on the stress field (stress tensor) and surface orientation. Whether or not a surface slips depends upon its cohesive strength, if any, and the coefficient of static friction, μ. The coefficient of static friction, μ, is the value of T_s that causes slip on a cohesionless surface and is often referred to as the fault "strength" in earthquake focal mechanism analysis (e.g., Harmsen, 1994). Under most crustal conditions, faults with $T_s \geq 0.6$ are ideally oriented for slip (Byerlee, 1978). Analysis of slip tendency provides a way to assess which faults are near the ideal orientation for slip and are the most likely to be associated with zones of increased fracture density and enhanced fracture permeability.

Dilation Tendency

Dilation of fractures is largely controlled by the resolved normal stress, which is a function of lithostatic and tectonic stresses and fluid pressure. The normal stress that a fracture feels depends on the magnitude and direction of the principal stresses relative to the fracture plane. The ability of a fracture to dilate and transmit fluid is directly related to its aperture, which in turn is a function of the effective normal stress acting upon it. The magnitude of the normal stress can be computed for surfaces of all orientations within a known or hypothesized stress field. This normal stress can be normalized by comparison with differential stress. The resulting dilation tendency (T_d) for a surface is then defined as

$$T_d = (\sigma_1 - \sigma_n) / (\sigma_1 - \sigma_3)$$

where σ_1 is the maximum principal compressive stress, and σ_3 is the minimum principal compressive stress.

BULK TRANSMISSIVITY ANISOTROPY

A population of steep, aligned, relatively permeable faults and fractures cutting a less permeable rock mass will tend to orient the maximum directional transmissivity parallel to the structural grain. In the case of unequal horizontal stresses acting on a population of steep faults and fractures, those with strikes *parallel* to the maximum horizontal compressive stress tend to open. Those with strikes *perpendicular* to the maximum horizontal stress tend to close. Similarly, some faults in an anisotropic stress field will be more ideally oriented for slip and others for locking. Thus, even if fault and fracture orientation distribution is isotropic, transmissivity in the maximum horizontal stress

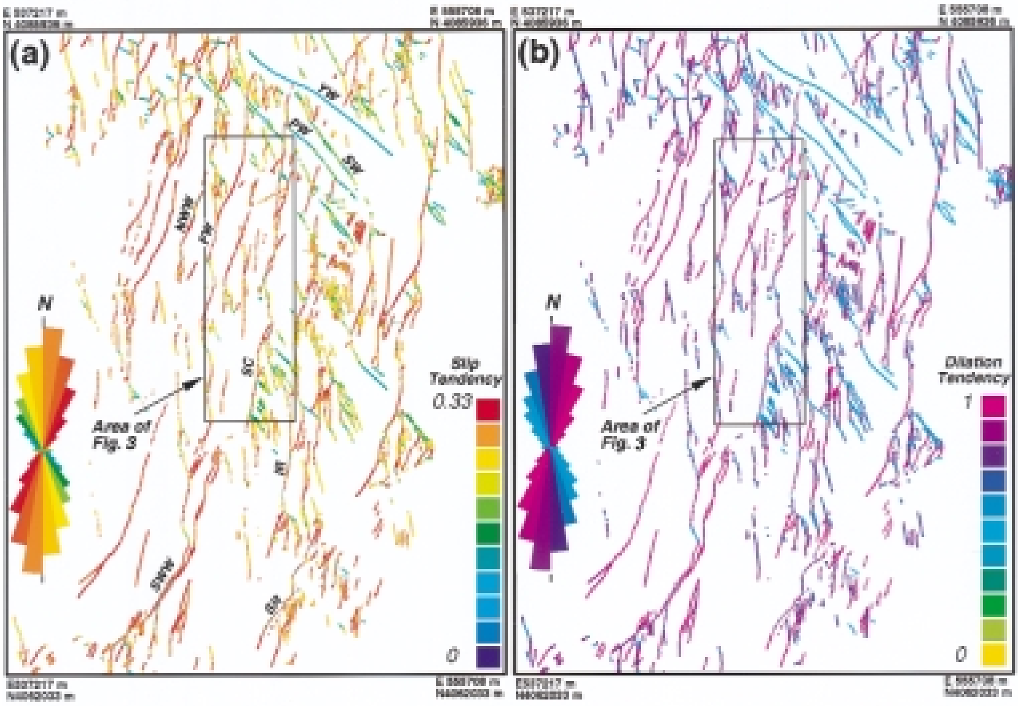

Figure 4. (a) Slip tendency map of Yucca Mountain faults mapped by Simonds et al. (1995). The rose diagram shows cumulative fault length in 10° strike azimuth bins. The map and rose diagram are colored according to slip tendency as shown by the slip-tendency plot and the color bar in Figure 3b. The area is as shown in Figure 1. Named faults discussed in the text are labeled on the map: NWW—Northern Windy Wash, SWW—Southern Windy Wash, FW—Fatigue Wash, SC—Solitario Canyon, IR—Iron Ridge, SR—Stagecoach Road, PW—Pagany Wash, SW—Sever Wash, and YW—Yucca Wash. (b) Dilation tendency map of Yucca Mountain faults. The map and rose diagram are colored according to dilation tendency as shown by the dilation-tendency plot and color bar in Figure 3c. The area is as shown in Figure 1.

direction can be enhanced, producing transmissivity anisotropy.

Because fault and fracture populations commonly exhibit preferred orientations and in situ horizontal stresses are commonly unequal, both are likely to occur together in nature and lead to anisotropic transmissivity. For example, in cases where σ_3 is horizontal, vertical faults and fractures perpendicular to σ_3 have the highest dilation tendency and are likely to be more conductive than those in other orientations (Fig. 2a). Faults and shear fractures are sensitive to the σ_1 direction and commonly form two conjugate sets intersecting at an acute angle (~60) centered on σ_1 (Fig. 2, b and c). In normal fault regimes where σ_1 is vertical, two sets of opposite-dipping conjugate normal faults commonly develop (Fig. 2b). In strike-slip fault regimes where σ_1 is horizontal, two sets of vertical conjugate strike-slip faults commonly develop (Fig. 2c). In areas where σ_3 is horizontal, fault and fracture preferred orientations, and slip tendency and dilation tendency all promote development of a net bulk transmissivity anisotropy with a maximum horizontal transmissivity perpendicular to σ_3 (Fig. 2d). The interaction of aquifer transmissivity with faults and fractures can be field tested by aquifer pumping tests. As done below, the results can be used to determine the full transmissivity tensor and to compare the orientation of the principal components of this tensor with the maximum and minimum in situ horizontal stress orientations and the distribution of faults and fractures.

PREDICTION OF ANISOTROPIC TRANSMISSIVITY AT YUCCA MOUNTAIN

The pattern of faults and fractures in the Yucca Mountain region (Fig. 1) resulted from deformation in a regional stress field that evolved from east-west extension before 10 Ma to west-northwest–east-southeast extension after 10 Ma (Zoback et al., 1981), and from thermoelastic contraction during cooling of the ash-flow tuffs (Sweetkind and Williams-Stroud, 1996). The result is a dominant population of north-south to northeast-southwest–trending normal faults, a subordinate population of northwest-southeast–trending strike-slip faults, and a group of minor connecting faults and curved fault tips (Day et al., 1998b; Ferrill et al., 1999). Fault growth by connection of overlapping fault segments produced irregular fault traces with cusps at fault intersections (Fig. 3a). Although faults at Yucca Mountain are related to several deformational episodes, some faults are unlikely to slip because of unfavorable orientations relative to the contemporary stress state.

Yucca Mountain lies within the western Basin and Range in a region characterized by both normal and strike-slip earthquakes. The regional occurrence of both normal and strike-slip earthquakes indicates that the maximum (σ_1) and intermediate (σ_2) principal compressive stresses have similar magnitudes (Zoback, 1992; Zoback et al., 1992). The least principal compressive stress (σ_3) is approximately horizontal and trends west-northwest–east-southeast. Therefore, σ_3 is the "odd axis" (Krantz, 1988) and has the most direct control on the pattern of fault slip tendency. Stock et al. (1985) estimated the following effective principal stresses at Yucca Mountain (corrected for fluid pressure) at a depth of 1 km: σ_1 = vertical = 21 MPa, σ_2 = N25°–30°E = 17 MPa, and σ_3 = N60°–65°W = 11 MPa for the region.

Slip-Tendency Analysis of Yucca Mountain Faults

Slip-tendency analysis of Yucca Mountain faults was performed using the relative stress values of Stock et al. (1985) given above, a three-dimensional fault model for western Yucca Mountain (Fig. 3b), and the faults mapped by Simonds et al. (1995; Fig. 4a). Faults that strike parallel to the north-northeast–trending maximum horizontal stress (025–030; 028 in Figs. 3 and 4) and dip 55° have the maximum slip tendencies. Slip tendencies are also near maximum (>0.3) for faults that are moderately to steeply dipping (40°–65°), and north-south to northeast-southwest (000–055) striking. Faults at 1 km depth have moderate slip tendencies relative to typical failure conditions. In contrast, at depths of earthquake rupture initiation (e.g., 5–15 km), stresses resolved on similarly oriented faults produce near-failure slip tendencies (Morris et al., 1996). As described by Harmsen (1994), the pattern of slipped faults in the Little Skull Mountain (Fig. 1) earthquake sequence is dominated by dip-slip on southeast-dipping normal faults and right-lateral strike-slip on vertical north-south trending

Stressed Rock *continued on p. 6*

Stressed Rock *continued from p. 5*

faults. This is the pattern predicted by slip tendency analysis of the Yucca Mountain stress field and supports simultaneous activity of strike-slip and normal faults in this area (Morris et al., 1996).

Examination of the faults mapped by Simonds et al. (1995) reveals that nearly all faults with known or suspected late Quaternary displacement are in orientations of high slip tendency (Fig. 4a). Some noteworthy examples are the Northern and Southern Windy Wash, Fatigue Wash, Solitario Canyon, Iron Ridge, and Stagecoach Road faults (Fig. 4a). In contrast, the northwest-southeast–trending Pagany Wash, Sever Wash, and Yucca Wash faults are in low slip-tendency orientations (Fig. 4a) and lack evidence of late Quaternary slip (Simonds et al., 1995).

Dilation-Tendency Analysis of Yucca Mountain Faults

Dilation-tendency analysis of faults and associated fractures at Yucca Mountain (e.g., Figs. 3c and 4b) was performed assuming the same relative stresses and mapped faults used for slip-tendency analysis. The results show that vertical faults and fractures that strike parallel to the maximum horizontal stress (025–030; 028 in Figs. 3 and 4) have the maximum dilation tendencies. Faults trending 028 ± 35° and dipping 65° to 90° have dilation tendencies of 0.8 or greater in the present stress field (Fig. 3c). Dilation-tendency analysis of faults at Yucca Mountain illustrates an abundance of steeply dipping north-northeast–trending faults that have high dilation tendency.

Implications for Anisotropic Transmissivity at Yucca Mountain

Faults with favorable orientations for slip or dilation present potential flow pathways. Although we explicitly consider only large map-scale faults, the processes that alter permeability of large faults and fracture systems also apply to abundant smaller scale fractures and faults like those seen in outcrops, boreholes, and the Exploratory Studies Facility (cf. Sweetkind and Williams-Stroud, 1996), resulting in an effective hydraulic continuum. The dominant trend of faults at Yucca Mountain is approximately north-south (005; see rose diagrams in Fig. 4). The strike, maximum slip tendencies, and maximum dilation tendencies of the fault population indicate the possibility of anisotropic transmissivity, with the direction of maximum transmissivity in the azimuth range between 005 (based on dominant fault trend) and 030 (based on slip- and dilation-tendency constraints).

TABLE 1. **DIRECTIONAL HYDRAULIC DIFFUSIVITIES ESTIMATED FOR OBSERVATION WELLS FROM LONG-TERM PUMPING TEST AT C-WELLS**

Well I.D.	Direction azimuth (θ)	Distance from pumped well (m)	Bulk aquifer transmissivity (m^2/d)	Square root of directional hydraulic diffusivity [$\sqrt{D(\theta)}$; $m/d^{1/2}$]
USW H-4	310	2245	670	560
ONC-1	327	843	1340	416
UE-25 WT #3	161	3526	1230	506
UE-25 WT #14	050	2249	1370	980

ESTIMATION OF ANISOTROPIC TRANSMISSIVITY AT YUCCA MOUNTAIN

A long-term aquifer pumping test was conducted at the C-well complex on the eastern flank of Yucca Mountain from May 1996 to March 1997 (Geldon et al., 1997). The C-well complex consists of three wells (UE-25c #1, UE-25c #2, and UE-25c #3) that are separated by distances of 30–77 m and form a right triangle. During this aquifer test, well UE-25c #3 was pumped at a rate of 9.5 L/s. Water levels in four observation wells (USW H-4, ONC-1, UE-25 WT #3, and UE-25 WT #14; Fig. 1), located at distances of 0.84–3.5 km, were monitored at 15 min intervals.

We estimated horizontal anisotropy of aquifer transmissivity on the basis of data from the four distant observation wells, using the method of Papadopulos (1965) for homogenous, anisotropic aquifers of infinite areal extent. Data from two other wells (UE-25c #1 and UE-25c #2) were not used because of complications related to their proximity to the pumped well. The technique requires the following data from at least three observation wells: (1) the directional azimuth (θ) to the monitored well from the pumped well; (2) bulk aquifer transmissivity (a scalar quantity equal to the geometric mean of the minimum and maximum directional transmissivities); and (3) the directional hydraulic diffusivity (a vector quantity). Directional hydraulic diffusivity [$D(\theta)$] is defined as the directional transmissivity [$T(\theta)$; a vector quantity] divided by the dimensionless bulk aquifer storage coefficient (S). Although we are primarily interested in $T(\theta)$, neither it nor S can be estimated separately from $D(\theta)$ until both the ratio of maximum to minimum $D(\theta)$ and the direction of maximum $D(\theta)$ are known. These are determined by fitting an ellipse to a polar plot of the square root of $D(\theta)$.

Our analysis differs in two ways from the interpretation of Geldon et al. (1997). First, we performed a two-step correction that accounts for the influence on water levels exerted by both direct borehole coupling to atmospheric pressure changes and the delayed atmospheric pressure signal that arrives through the overlying geologic formation. Second, we assume that S is constant throughout the aquifer, and thus differences in $D(\theta)$ between observation wells are attributed to $T(\theta)$. The bulk aquifer transmissivity estimates obtained from our analysis (Table 1) are broadly consistent with, but less variable than those in Geldon et al. (1997).

We began our analysis of aquifer anisotropy by testing the assumption of a homogenous aquifer system. In a purely homogenous aquifer, the bulk transmissivity estimates obtained from each observation well should be the same. With the exception of well USW H-4, aquifer transmissivity estimates are quite similar (Table 1). Because the transmissivity estimate for well USW H-4 could be affected by a fault system between it and the pumped well, this well was excluded from the analysis of horizontal anisotropy. A polar plot of the square root of $D(\theta)$ for the remaining three wells shows that an exact-fitting ellipse could not be obtained from the data, consistent with the fact that not every set of three points defines an ellipse (Fig. 5).

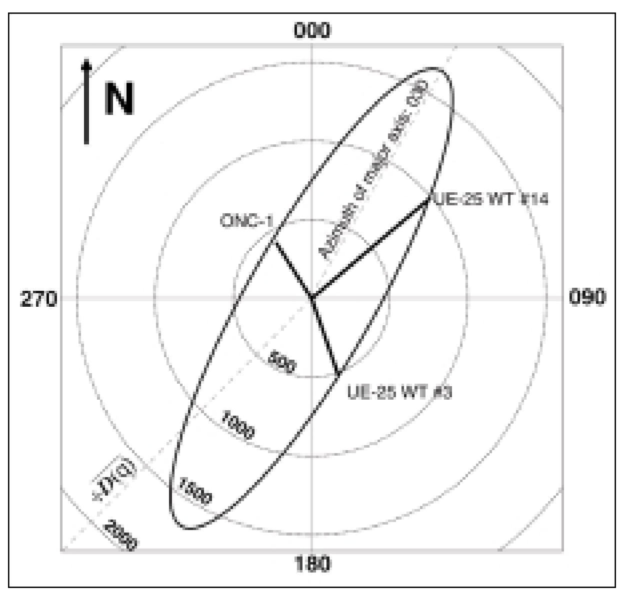

Figure 5. An ellipse with major semi-axis oriented 030 provides a close match to directional hydraulic diffusivities and indicates anisotropic transmissivity that is consistent with predictions based on fault and fracture orientations and effects of regional stress. Concentric contours are in m/$d^{1/2}$.

Although the ellipse in Figure 5 is not an exact fit, it closely matches the observation well data with major semi-axis oriented 030. Because of uncertainty associated with aquifer pumping tests, and the limitation of having only the minimum number of data points to constrain an ellipse, the ratio of minimum to maximum directional transmissivity is poorly constrained. With this in mind, we estimate from Figure 5 a maximum $T(\theta)$ of 5400 m^2/d (azimuth 030), a minimum $T(\theta)$ of 315 m^2/d (azimuth 120), and a bulk S value of 0.002. This analysis indicates a northeast trend in the direction of maximum $T(\theta)$ consistent with the north-northeast (025–030) trend inferred from the slip and dilation tendency.

IMPLICATIONS FOR PROPOSED YUCCA MOUNTAIN REPOSITORY SITE

Current groundwater flow models at Yucca Mountain (e.g., Czarnecki et al., 1997, Department of Energy, 1998a, 1998b) do not incorporate anisotropy of transmissivity. A flow pattern parallel to the hydraulic gradient, as expected in an isotropic aquifer (Freeze and Cherry, 1979), would result in relatively short southeast-directed travel distances in the unconfined welded-tuff aquifer before the flow enters alluvial deposits. In contrast, by taking into account the orientation of maximum horizontal transmissivity and the inferred presence of fault- and fracture-controlled flow conduits, we propose a model in which more southward-directed flow paths would increase travel distances in the tuff aquifer and reduce the amount of flow in alluvium between Yucca Mountain and the receptor location. Such a difference in direction is important, because relative flow velocities should be faster in the lower porosity tuff aquifer, and sorption of radionuclides should be less in the tuff, owing to its lower surface area of sorbing mineral grains (e.g., clays, iron oxides, and calcite).

CONCLUSIONS

In the contemporary stress state at 1 km depth at Yucca Mountain, slip and dilation tendency analyses indicate the following: faults that strike north-northeast (000–055) and dip 40°–65° have high slip tendencies, the maximum being for faults that strike north-northeast (025–030) and dip 53°; and faults that strike north-northeast (350–065) and dip 65°–90° have high dilation tendencies, the maximum being for vertical faults that strike north-northeast (025–030).

The dominant north-south (~005) trend of faults at Yucca Mountain, coupled with slip-tendency and dilation-tendency considerations suggest anisotropic transmissivity, with maximum transmissivity in the azimuth range between 005 and 030.

The anisotropic transmissivity estimated at Yucca Mountain has a maximum principal direction of approximately 030, consistent with the hypothesis that anisotropy is controlled by faults and fractures in the present-day in situ stress field.

Note: For more information on the Yucca Mountain site, see www.ymp.gov/va.htm.

About People

GSA Member Stephen W. Forster, Federal Highway Administration, Centreville, Virginia, received the 1998 Prevost Hubbard Award from American Society of Testing and Materials Committee D-4 on Road and Paving Materials.

Fellow Lee C. Gerhard, state geologist and director of the Kansas Geological Survey, has been made an honorary member of the Kansas Geological Society.

Fellow Syed E. Hasan, University of Missouri—Kansas City, has received the Claire P. Holdredge Award from the Association of Engineering Geologists.

Fellow Holly Stein, Colorado State University, Fort Collins, has been awarded a Fulbright Research Fellowship to the Norwegian University of Science and Technology.

The Woods Hole Oceanographic Institution has awarded the Henry Bryant Bigelow Chair to Fellow Brian E. Tucholke.

Member Owen L. White, Toronto, Ontario, has received the Hans Cloos Medal from the Canadian National Group of the International Association for Engineering Geology and the Environment.

ACKNOWLEDGMENTS

This paper resulted from work at the Center for Nuclear Waste Regulatory Analyses (CNWRA) for the U.S. Nuclear Regulatory Commission (NRC) under contract NRC-02-97-009. The paper is an independent product of CNWRA and does not necessarily reflect the views or regulatory position of the NRC. Ferrill and Morris thank co-developers (D. Brent Henderson, Budhi Sagar, Josh Buckner, Robert Boenau, Scott Walnum, Chad Fleming, and Goodluck Ofoegbu) of the 3DStress™ version 1.3 stress analysis program that was used for slip-tendency and dilation-tendency analyses. We thank Annette Mandujano for assistance in manuscript preparation. John Stamatakos, Britt Hill, Larry McKague, and Budhi Sagar provided helpful suggestions and technical reviews, Bret Leslie, Jeffrey Ciocco, Neil Coleman, and Phil Justus of the NRC provided valuable technical comments; and Suzanne Kay, Grady O'Brien, David Vaniman, Mary Lou Zoback, and Claudia Faunt provided further comments.

REFERENCES CITED

Barton, C. A., Zoback, M. D., and Moos, D., 1995, Fluid flow along potentially active faults in crystalline rock: Geology, v. 23, p. 683–686.

Bredehoeft, J. D., 1997, Fault permeability near Yucca Mountain: Water Resources Research, v. 33, p. 2459–2463.

Byerlee, J. D., 1978, Friction of rocks: Pure and Applied Geophysics, v. 116, p. 615–626.

Carlsson, A., and Olsson, T., 1979, Hydraulic conductivity and its stress dependence: Proceedings, Paris, Workshop on Low-Flow, Low-Permeability Measurements in Largely Impermeable Rocks, p. 249–259.

Czarnecki, J. B., Faunt, C. C., Gable, C. W., and Zyvoloski, G. A., 1997, Hydrogeology and preliminary calibration of a preliminary three-dimensional finite-element ground-water flow model of the site saturated zone, Yucca Mountain, Nevada: U.S. Geological Survey, Yucca Mountain Project Milestone Report SP23NM3.

Day, W. C., Potter, C. J., Sweetkind, D., Dickerson, R. P., and San Juan, C. A., 1998a, Bedrock geologic map of the Central Block area, Yucca Mountain, Nye County, Nevada: U.S. Geological Survey Miscellaneous Investigations Series Map I-2601, scale 1:6000.

Day, W. C., Dickerson, R. P., Potter, C. J., Sweetkind, D. S., San Juan, C. A., Drake, R. M. II, and Fridrich, C. J., 1998b, Geologic map of the Yucca Mountain area, Nye County, Nevada: U.S. Geological Survey Geological Investigations Series I-2627, scale 1:24,000.

Dudley, W. W., and Larson, J. D., 1976, Effect of irrigation pumping on the desert pupfish habitat in Ash Meadows, Nye County, Nevada: Geological Survey Professional Paper 927.

Fabryka-Martin, J. T., Wolfsberg, A. V., Levy, S. S., Campbell, K., Tseng, P., Roach, J. L., and Wolfsberg, L. E., 1998, Evaluation of flow and transport models of Yucca Mountain, based on chlorine-36 studies for FY98: Los Alamos National Laboratory, Yucca Mountain Project Milestone Report SP33DDM4.

Ferrill, D. A., Morris, A. P., Jones, S. M., and Stamatakos, J. A., 1998, Extensional layer-parallel shear and normal faulting: Journal of Structural Geology, v. 20, p. 355–362.

Ferrill, D. A., Stamatakos, J. A., and Sims, D., 1999, Normal fault corrugation: Implications for growth and seismicity of active normal faults: Journal of Structural Geology (in press).

Finkbeiner, T., Barton, C. A., and Zoback, M. D., 1997, Relationships among in-situ stress, fractures and faults, and fluid flow: Monterey Formation, Santa Maria Basin, California: American Association of Petroleum Geologists Bulletin, v. 81, p. 1975–1999.

Freeze, R. A., and Cherry, J. A., 1979, Groundwater: Englewood Cliffs, New Jersey, Prentice-Hall, Inc., 604 p.

Fridrich, C. J., Dudley, W. W., Jr., and Stuckless, J. S., 1994, Hydrogeologic analysis of the saturated-zone ground-water system, under Yucca Mountain, Nevada: Journal of Hydrology, v. 154, p. 133–168.

Geldon, A. L., Umari, A. M. A., Fahy, M. F., Earle, J. D., Gemmel, J. M., and Darnell, J., 1997, Results of hydraulic and conservative tracer tests in Miocene tuffaceous rocks at the C-Hole Complex, 1995 to 1997, Yucca Mountain, Nevada: U.S. Geological Survey Yucca Mountain Milestone Report SP23PM3.

Harmsen, S. C., 1994, The Little Skull Mountain earthquake of 29 June 1992: Aftershock focal mechanisms

Stressed Rock *continued on p. 8*

GSA ANNUAL MEETING *Crossing Divides*

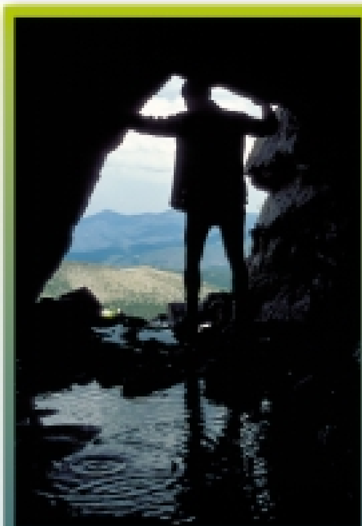

1999
October 25–28

Denver, Colorado

Colorado Convention Center
Hyatt Regency Hotel
Marriott City Center Hotel

www.geosociety.org/meetings/99

Abstracts due: *July 12*

General Co-Chairs:	Technical Program Co-Chairs:	Field Trip Co-Chairs:
Mary J. Kraus and David Budd, *University of Colorado*	**Craig Jones and G. Lang Farmer,** *University of Colorado*	**Alan Lester and Bruce Trudgill,** *University of Colorado*

Proposal deadlines for both technical program and field trips have passed.

Pardee Keynote Sessions
(all invited speakers)

- **K01 Impact Events: Environmental Consequences and Their Influence on the Origin and Evolution of Life**
- **K02 Human Transformation of the Physical Landscape**
- **K03 Maintaining a Livable Earth: Conversations Among Concerned Geologists**
- **K04 Geoscientists in the Legal System: The Challenge for the Next Century**
- **K05 Low-Latitude Precambrian Glaciation: Geochemical, Climatic, and Biological Effects of the Snowball Earth**
- **K06 Globally Warm Climates of the Early Cenozoic: Evidence, Causes, and Biotic Consequences**
- **K07 The Case for Steady-State Mountain Belts: Observations, Models, and Implications for Global Tectonics**
- **K08 New Insights on Organic Metamorphism in the Earth**

Stressed Rock *continued from p. 7*

and tectonic stress field implications: Seismological Society of America Bulletin, v. 84, p. 1484–1505.

Jaeger, J. C., and Cook, N. G. W., 1979, Fundamentals of rock mechanics (third edition): London, Chapman and Hall, 593 p.

Krantz, R. W., 1988, Multiple fault sets and three-dimensional strain: Theory and application: Journal of Structural Geology, v. 10, p. 225–237.

Levy, S. S., Sweetkind, D. S., Fabryka-Martin, J. T., Dixon, P. R., Roach, J. L., Wolfsberg, L. E., Elmore, D., and Sharma, P., 1997, Investigations of structural controls and mineralogic associations of Chlorine-36 fast pathways in the ESF: Los Alamos National Laboratory, Yucca Mountain Project Milestone Report SP2301M4.

Morris, A. P., Ferrill, D. A., and Henderson, D. B., 1996, Slip-tendency analysis and fault reactivation: Geology, v. 24, p. 275–278.

National Research Council, 1996, Rock fractures and fluid flow: Washington, D.C., National Academy Press, 551 p.

Papadopulos, I. S., 1965, Nonsteady flow to a well in an infinite anisotropic aquifer: International Symposium of Scientific Hydrology, Proceedings, Dubrovnik Symposium on the Hydrology of Fractured Rocks, p. 21–31.

Sass, J. H., Dudley, W. W., Jr., and Lachenbruch, A. H., 1995, Regional thermal setting, *in* Oliver, H. W., et al., eds., Major results of geophysical investigations at Yucca Mountain and vicinity, southern Nevada: U.S. Geological Survey Open-File Report 95-74, 23 p.

Simonds, W. F., Whitney, J. W., Fox, K., Ramelli, A., Yount, J. C., Carr, M. D., Menges, C. D., Dickerson, R., and Scott, R. B., 1995, Map of fault activity of the Yucca Mountain area, Nye County, Nevada: U.S. Geological Survey Miscellaneous Investigations Series Map I-2520, scale 1:24,000.

Stock, J. M., Healy, J. H., Hickman, S. H., and Zoback, M. D., 1985, Hydraulic fracturing stress measurements at Yucca Mountain, Nevada, and relationship to regional stress field: Journal of Geophysical Research, v. 90, p. 8691–8706.

Sweetkind, D. S., and Williams-Stroud, S. C., 1996, Characteristics of fractures at Yucca Mountain, Nevada: Synthesis report: Denver, Colorado, U.S. Geological Survey Administrative Report.

U.S. Department of Energy, 1998a, Viability assessment of a repository at Yucca Mountain: Introduction and site characteristics, December 1998. Volume 1: Las Vegas, Nevada, U.S. Department of Energy, Office of Civilian Radioactive Waste Management, DOE/RW-0508.

U.S. Department of Energy, 1998b, Viability assessment of a repository at Yucca Mountain: Total system performance assessment, December 1998. Volume 3: Las Vegas, Nevada, U.S. Department of Energy, Office of Civilian Radioactive Waste Management, DOE/RW-0508.

Waddell, R. K., 1982, Two-dimensional, steady-state model of ground-water flow, Nevada Test Site and vicinity, Nevada-California: U.S. Geological Survey Water Resources Investigations Report 82-4085.

Winograd, I. J., and Thordarson, W., 1975, Hydrogeologic and hydrochemical framework, south-central Great Basin, Nevada-California, with special reference to the Nevada Test Site: U.S. Geological Survey Professional Paper 712-C.

Zoback, M. L., 1992, First- and second-order patterns of stress in the lithosphere: The world stress map project: Journal of Geophysical Research, v. 97(B8), p. 11,703–11,728.

Zoback, M. L., Anderson, R. E., and Thompson, G. A., 1981, Cenozoic evolution of the state of stress and style of tectonism of the Basin and Range Province of the western United States: Royal Society of London Philosophical Transactions, sec. A, v. 300, p. 407–434.

Zoback, M. L., and 36 project participants, 1992, World stress map—Maximum horizontal stress orientations: Journal of Geophysical Research, v. 87(B8).

Manuscript received December 20, 1998; accepted March 10, 1999. ■